

Experimental and Theoretical Studies of Gas Phase Ion Mobility and Energetics: Protonated Saturated and Unsaturated Aldehydes in Helium

M. Omezzine Gnioua,^{1,2} A. Spesyvyi,¹ and P. Španěl¹

¹ J. Heyrovsky Institute of Physical Chemistry, Academy of Sciences of the Czech Republic, Prague, Czechia.

² Charles University Prague, Faculty of Mathematics and Physics, Prague, Czechia.

Abstract. Theoretical calculations and experimental measurements were carried out for selected classes of volatile organic compounds (VOC) to further understand the ion–molecule reactions important for mass spectrometric trace gas analysis. Quantum chemistry calculations based on the density functional theory, DFT, were performed using the ORCA software to study the structures and energetics of protonated aldehyde ions. The total enthalpies of the neutral and protonated molecules were calculated at the B3LYP 6-311++G(d,p) level of theory including the D4 dispersion correction for the standard temperature and pressure. Proton affinities were thus obtained for pentanal, heptanal, octanal, 2-pentenal, 2-heptenal and 2-octenal. The Selected Ion Flow Drift Tube Mass Spectrometry (SIFDT-MS) was used to measure the mobilities and energies of protonated aldehyde ions under different reduced electric field intensities (E/N) and the results were compared with theoretical values based on the calculated ion geometries.

Introduction

Mobility measurements have long been recognized as a valuable method of gaining information about interactions of ions with gaseous atoms and molecules.[*Ellis, et al.*, 1978; *McDaniel and Mason*, 1973] In selected ion flow tube drift mass spectrometry, SIFDT-MS, [*Spesyvyi, et al.*, 2021; *Tichý, et al.*, 1987] ions drift through a region filled with a homogenous buffer gas. Under the influence of an electric field, the ions acquire drift velocity v_d that is directly proportional to the electric field intensity E

$$v_d = \mu E, \quad (1)$$

where the coefficient μ is called the ion mobility and depends on the composition of the ions and the buffer gas. The mobility is therefore a property that provides information on the magnitude of ion–neutral interactions experienced by ions as they travel through a buffer gas.

The basic principles of SIFDT-MS have been well-established for years [*Tichý et al.*, 1987] so only essential features as they pertain to the present instrument will be given here. H_3O^+ ions are generated in the ion source using a hollow cathode (HC) [*Spesyvyi, et al.*, 2021] containing water vapour at concentrations high enough so that H_2O ions are quantitatively converted into H_3O^+ ions still within the ion source. The reagent ions are formed from vapours of volatile organic compounds, VOC, introduced via an inlet port into the ion source where they react with H_3O^+ producing protonated organic ions. After extraction of the ions from the source, they are introduced into the upstream quadrupole mass spectrometer for selection according to their mass-to-charge ratio and injected into a flow drift tube reactor (DTR) through a venturi inlet. A fast-flowing helium buffer gas enters the tube which convicts them along the flow tube into the drift-reaction region where a uniform electric field is applied along the axis of the tube. The ions are transported through the DTR region by a combination of electric-field-induced drift by the buffer gas. At the end of the DTR, the ions are sampled through a nose cone, analysed according to their m/z by quadrupole mass spectrometer and counted by an electron multiplier. The ion gates are installed in the DTR so that the residence time and hence drift velocity and mobility of ions in the electric field can be determined.

The actual value of the near-zero-field mobility for a given ion drifting through a buffer gas is entirely dependent on the form of the interaction potential between the ion and the atoms of the buffer gas. However, the main objective of this theory is to use the Viehland and Mason theory combined with the de Gouw et al. approach to estimate the parameters of the (12, 4) interaction potential to calculate the ion mobilities based on hard sphere repulsion and an induced-dipole polarization attraction.[*Dryahina and Španěl*, 2005] The used (12, 4) model of an ion–neutral molecule interaction represents the interaction potential between an ion and a carrier gas atom $V(r)$ expressed as a function of their distance as a sum of one repulsive term and one attractive term:

$$V(r) = \frac{B}{r^{12}} - \frac{C_4}{r^4}, \quad (2)$$

where the attractive term C_4/r^4 describes the long-range charge/induced dipole interactions between the ions and the carrier gas atoms governed by polarizability of He atoms (0.204 Å^3) and the repulsive term B/r^{12} is an approximate representation of the short-range repulsive barrier which is determined from the average hard sphere

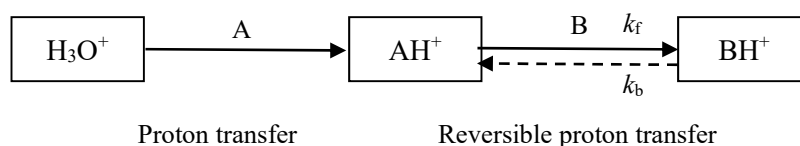


Figure 1. Ion chemistry of H_3O^+ with molecules A and B.

radius of the ion calculated from its geometry. The calculation is carried out in several steps: first, the geometry of the molecular ion is determined, then the mean geometrical cross-section for hard-sphere collisions is calculated, and finally, mobility is obtained from the approximate interaction potential parameterised using this hard-sphere cross-section. Details of these calculation steps are given [Dryahina and Španěl, 2005].

One of the most important gas phase ion–molecule reaction types in soft chemical ionisation mass spectrometry is the proton transfer. H_3O^+ is a widely used reagent ion in SIFT-MS and PTR-MS and it is also a core to hydrated clusters involved in SESI-MS to trace gas analysis of VOC [Bruderer *et al.*, 2019]. The proton transfer reactions are known to be fast, proceeding at the collisional rate, when they are exothermic [Bouchoux *et al.*, 1996]. As the thermicity of these reactions is defined by a difference in proton affinities, PA, between the donor molecule (H_2O in this case) and the acceptor molecule (A), it is very important to have reliable values of PA for the VOC molecules encountered in practical analyses. H_3O^+ thus reacts with a volatile organic compound, A, by exothermic proton transfer forming the AH^+ ions, as long as PA of A is greater than PA of H_2O ($691 \text{ kJ}\cdot\text{mol}^{-1}$). [Hunter and Lias, 1998; Lias *et al.*, 2016]. In the presence of another volatile organic compound B with even greater PA, AH^+ ions may react via proton transfer reaction with a rate coefficient k_f to form BH^+ ions. Figure 1 shows a scheme of the reaction system of H_3O^+ , A and B.

When the PA of A and B are close to each other, the reverse proton transfer reaction can take place with rate coefficient, k_b (see Figure 1) [Tichy *et al.*, 1989].

The equilibrium rate constant can be then defined as:

$$K = \frac{k_f}{k_b}. \quad (3)$$

Based on the thermodynamics principles, K is related to the Gibbs free energy change (ΔG) in a reaction and the temperature T by an exponential equation

$$K = e^{\left(\frac{-\Delta G}{k_B T}\right)}, \quad (4)$$

where k_B is the Boltzmann constant. Note that (ΔG) is expressed as

$$\Delta G = \Delta H - T\Delta S, \quad (5)$$

where ΔH is the enthalpy change corresponding to the difference in PA of A and B and ΔS is the entropy change that can be calculated from the partition functions based on the available degrees of freedom.

A large number of PA values is collected in the NIST webbook database [Linstrom and Mallard, 2011] and most of them are taken from an evaluation review [Hunter and Lias, 1998]. However, values for many VOCs are missing and the accuracy of those available is sometimes questionable. Therefore, with the advance in computational chemistry methods, it should be possible to reliably calculate PA values for all VOC molecules. In the present study, we intend to demonstrate that such calculations are feasible using the density functional theory, DFT, as implemented in the freely available software package ORCA. Note that DFT is one of the most convenient methods for quantum chemistry calculations of the structure of atoms, molecules, crystals, surfaces, and their interactions. It can predict a wide variety of molecular properties for unknown systems without any experimental input with low computational effort required and is used for PA calculations by others [Etim, *et al.*, 2020].

Materials and methods

Computational methods

All quantum chemistry calculations were performed using ORCA 5.0.1 software.[Neese, 2018] Molecular geometries of the H_2O molecule and all six neutral aldehydes molecules and their protonated forms were first drawn using AVOGADRO [Hanwell *et al.*, 2012] software and then further optimised using ORCA with the B3LYP DFT and the basis set 6-311++G(d,p) with the D4 correction [Caldeweyher *et al.*, 2017]. Keeping in mind that dispersion correction may not be needed for our case whilst it is well suited for, weak Van der Waals and π – π interactions, in dimers and molecules with many functional groups. This level of theory was also used to calculate the normal mode vibrational frequencies and thermodynamic quantities of the neutral molecules and the

ion structures. The total enthalpies of all neutral molecules and ions were thus calculated for the standard temperature and pressure (298.15 K, 1013.25 mbar). The calculations were performed for the most feasible structure of the ions, obtained by placing the H^+ proton near the oxygen site of the aldehyde molecule.

Enthalpies were calculated as the sum of the total electronic energy, E_{el} , the zero-point vibrational energy, E_{ZPV} , the temperature-dependent portion of the vibrational energy, $E_{vib}(T)$ and the thermal translational and rotational energies ($5/2RT$) of the molecule at 298 K.

$$H = E_{el} + E_{ZPV} + E_{vib}(T) + 5/2RT \quad (6)$$

For this calculation to produce correct results, all vibrational frequencies calculated for the optimal geometry must be real and not imaginary.

Proton affinities, PA, are defined as the negative enthalpy change at 298 K for a notional reaction:



PAs were thus calculated as the difference between the total enthalpies of the neutral molecules and the corresponding protonated structures, accounting for the thermal enthalpy of a free proton of $6.2 \text{ kJ} \cdot \text{mol}^{-1}$ at 298.15 K according to the following expression:

$$PA = -\Delta H \quad (8)$$

The theoretical mobilities of protonated aldehydes in He were obtained using the *DiffusionCalc* program [Dryahina and Španěl, 2005] by averaging 200 random orientations of the calculated ion geometries.

SIFDT instrument

The ion mobility measurements were done using the SIFDT apparatus constructed and developed in our laboratory [Spesvyi, *et al.*, 2015; Spesvyi, *et al.*, 2021] that includes an octupole ion guide behind the ion source and an additional drift tube stage between the venturi injector and the main drift tube. Unique to this SIFDT instrument is the direct determination of the ion residence time in the reaction zone, which is achieved by utilizing Hadamard modulation of the injected ion current [Spesvyi and Španěl, 2015; Zare, *et al.*, 2003]. The ion source drift tube was removed for the present experiments. The schematic of the present configuration is shown in Figure 2. Water vapour is introduced into the hollow cathode HC discharge where H_3O^+ ions are produced. A small amount of a liquid VOC sample can be placed into a vial with a septum and the headspace consisting of saturated vapour is taken via a stainless-steel capillary and introduced via the VOC port into the ion source chamber where collisions with H_3O^+ take place producing protonated molecules mostly in octupole (OP) ion guide. The gas flow exits the ion source and is pumped by a booster port of a turbomolecular pump (Edwards nEXT300). The ions are then guided via the OP to the disk with a 2 mm central aperture into an upstream quadrupole mass filter (QMF). After selection by m/z in QMF, they are injected via the Venturi inlet (VI) to the short 15 mm Venturi flow-drift tube (VDT) with $E = 5 \text{ V cm}^{-1}$ (see Figure 2). The ion current can be precisely modulated at the exit of VDT by three grid electrodes. For the present experiments Hadamard sequence modulation is used to obtain ion arrival time distributions (ATD) at the downstream detector. The main drift tube reactor DTR, in which the ion–molecule reactions occur, is in the form of a resistive glass tube 145 mm long, 10 mm ID, as supplied by Photonis. At the end of this DTR there is a sampling nose cone (SNC) with a central 0.5 mm orifice through which the reagent and product ions are sampled into the downstream quadrupole mass analyser (QMA) and their count rates are detected

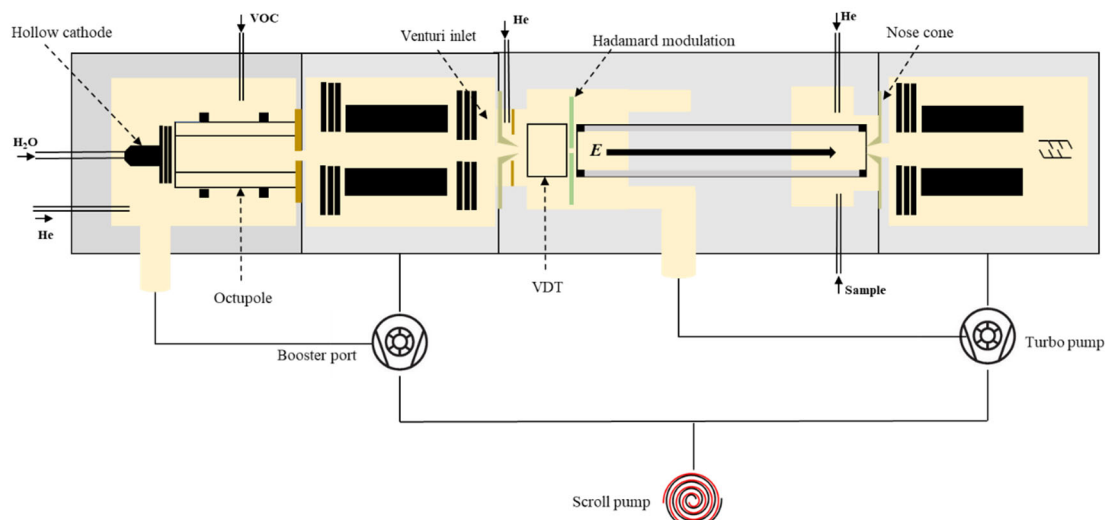


Figure 2. A schematic diagram of SIFDT-MS.

by the electron multiplier with a conversion dynode. Helium buffer gas and the sample gas are introduced into the DTR near the SNC and pumped along the DTR and exit before they can enter the VDT. This (counter) flow is in opposition to the direction of ion drift due to the axial E -field, which ensures that the composition of gas in DTR is homogeneous and is not affected by any gas from the VDT (see Figure 2). The DTR chamber is pumped by the valve-regulated booster port of the second Edwards nEXT300 turbomolecular pump (see Figure 2).

Reagents

The following reagents were used for the present study as purchased from Sigma Aldrich: pentanal (valeraldehyde 97 %), heptanal 95 %, octanal 99 %, trans-2-pentenal 95 % and trans-2-heptenal 97 %.

Results and discussion

Proton affinity

The DFT calculations of proton affinities were done for all six aldehyde molecules, Table 1 shows the optimized structures of the molecules and ions. The geometries of the neutral aldehydes agree well with the generally accepted structures [Kim, *et al.*, 2022] with minor differences due to the DFT optimisation. The geometries of the protonated aldehydes all show similar structure of the CHOH^+ group with the rest of the molecule similar to the neutral structure. The calculated proton affinities are listed in Table 2. Note that the PA calculated for H_2O differs from the NIST value ($691 \text{ kJ}\cdot\text{mol}^{-1}$) only by $3.5 \text{ kJ}\cdot\text{mol}^{-1}$ which is currently considered the state-of-the art so-called chemical accuracy ($\pm 1 \text{ kcal}\cdot\text{mol}^{-1} = 4 \text{ kJ}\cdot\text{mol}^{-1}$). The calculated PAs of the saturated aldehydes are very similar, within $3 \text{ kJ}\cdot\text{mol}^{-1}$ and they are all lower than the PAs for unsaturated aldehydes. The only value available in NIST is that for 1-pentanal ($796.6 \text{ kJ}\cdot\text{mol}^{-1}$) is only $2.6 \text{ kJ}\cdot\text{mol}^{-1}$ higher than our calculated value, again within the chemical accuracy. This indicates that our choice of the B3LYP functional, D4 dispersion correction and 6-311++G(d,p) basis set is suitable for accurate PA calculations. Note that the previous calculation of PA for octanal molecule computed using B3LYP/6-31+G(d, p) gave a value of $807 \text{ kJ}\cdot\text{mol}^{-1}$ close to our result [Bhatia, 2023].

Table 1. Optimised structures of the molecules and ions using the DFT B3LYP D4 6-311++G(d,p) theory.

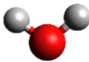
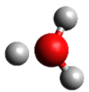
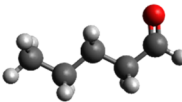
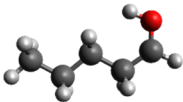
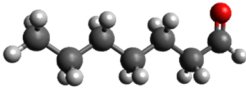
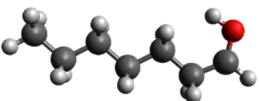
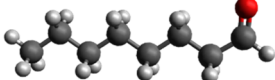
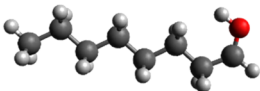
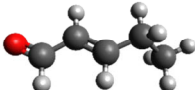
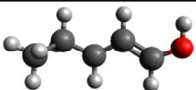
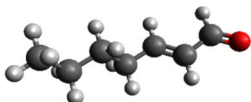
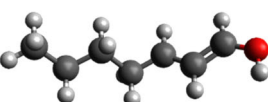
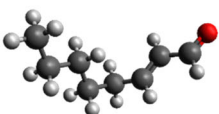
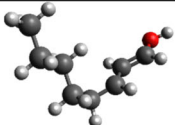
Compounds	Neutral Geometry M	Protonated Geometry MH^+
Water (H_2O)		
Pentanal ($\text{C}_5\text{H}_{10}\text{O}$)		
Heptanal ($\text{C}_7\text{H}_{14}\text{O}$)		
Octanal ($\text{C}_8\text{H}_{16}\text{O}$)		
2-Pentenal ($\text{C}_5\text{H}_8\text{O}$)		
2-Heptenal ($\text{C}_7\text{H}_{12}\text{O}$)		
2-Octenal ($\text{C}_8\text{H}_{14}\text{O}$)		

Table 2. PA ($\text{kJ}\cdot\text{mol}^{-1}$) values were calculated using the B3LYP 6-311++G(d,p) level of theory.

Compound M	Formula	PA, [$\text{kJ}\cdot\text{mol}^{-1}$]
Water	H_2O	687.5
Pentanal	$\text{C}_5\text{H}_{10}\text{O}$	794
Heptanal	$\text{C}_7\text{H}_{14}\text{O}$	797
Octanal	$\text{C}_8\text{H}_{16}\text{O}$	797
2-pentenal	$\text{C}_5\text{H}_8\text{O}$	844
2-heptenal	$\text{C}_7\text{H}_{12}\text{O}$	850
2-octenal	$\text{C}_8\text{H}_{14}\text{O}$	855

Table 3. Reduced mobilities of protonated ions at different E/N . ($1\text{Td} = 10^{-17} \text{ V}\cdot\text{cm}^2$).

E/N , [Td]	μ_0 , [$\text{cm}^2\cdot\text{V}^{-1}\cdot\text{s}^{-1}$]					
	Pentanal (m/z 87)	Heptanal (m/z 115)	Octanal (m/z 129)	2-pentenal (m/z 85)	2-heptenal (m/z 113)	2-octenal (m/z 127)
7	10.38			10.66		
8	10.29	8.74		10.91	8.49	
9	10.29	8.72	7.94	10.58	8.56	
10	10.23	8.70	7.89	10.51	8.35	7.46
11	10.19	8.68	7.90	10.47	8.38	7.72
12	10.19	8.49	7.93	10.40	8.36	7.78
13		8.65	7.84		8.33	7.58
14			7.86			7.33
15						7.37

Mobility

The ion mobilities measured for the protonated aldehydes at 2 mbar pressure in SIFDT were converted to reduced ion mobility values. This facilitates comparisons of ion mobilities obtained under different conditions. The reduced ion mobility μ_0 , is calculated from the value measured at buffer gas pressure p and temperature T by

$$\mu_0 = \mu \frac{p}{p_0} \frac{T_0}{T} \quad (9)$$

to correspond to the standard atmospheric pressure $p_0 = 1013.25$ mbar and temperature $T_0 = 273.15$ K. The experimentally obtained values are listed in Table 3 for the covered ranges of E/N . Note that the differences between the covered E/N ranges are due to different drift times, for heavier ions we had to use slightly stronger field.

The dependencies of reduced mobilities μ_0 on E/N for all studied protonated aldehydes are shown in Figure 3. It can be seen that in this low E/N range the μ_0 of the ions are almost constant. This means that the experimental conditions for the studied ions can be considered as the zero field approximation. Thus, we can use this data to derive zero field reduced ion mobility.

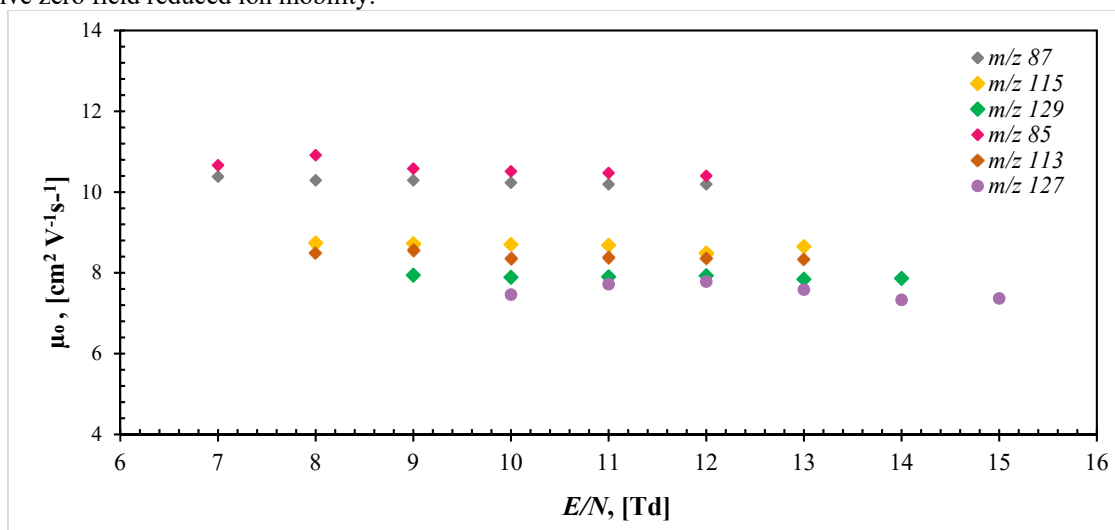

Figure 3. Mobility of protonated aldehydes in He as function of E/N at 2 mbar pressure.

Table 4. Reduced ion mobility calculated from the present SIFDT experimental measurements for the ions indicated compared with the theoretical values.

Ion	m/z	μ_0 [$\text{cm}^2 \cdot \text{V}^{-1} \cdot \text{s}^{-1}$]	
		Theory (12,4)	Experimental
$(\text{C}_5\text{H}_{10}\text{O})\text{H}^+$	87	10.34	10.24
$(\text{C}_7\text{H}_{14}\text{O})\text{H}^+$	115	8.63	8.65
$(\text{C}_8\text{H}_{16}\text{O})\text{H}^+$	129	7.97	7.88
$(\text{C}_5\text{H}_8\text{O})\text{H}^+$	85	10.04	10.54
$(\text{C}_7\text{H}_{12}\text{O})\text{H}^+$	113	8.67	8.39
$(\text{C}_8\text{H}_{14}\text{O})\text{H}^+$	127	7.86	7.51

In order to compare the extrapolated experimental zero-field mobilities with theoretical values, the slopes of plots of v_d as a function of E/N were calculated and converted to zero-field-mobilities given in Table 4 together with the theoretical values based on (12,4) potential. Note that they agree within 5%, this is a very good agreement given the approximations involved in the hard-sphere model.

Conclusion

The results from the present computational study are promising as they suggest the possibility of understanding the energetics of the reactions of hydronium ions, H_3O^+ with a volatile organic compound, VOC. This is important for SIFDT-MS for interpretation and understanding how to develop reliable quantification methods. We have now developed and tested a computational method to calculate proton affinities of the VOC molecules with chemical accuracy. These values will have to be validated experimentally by studying reversible proton transfer reactions [Tichy, *et al.*, 1989].

We have measured the reduced mobilities of protonated aldehydes in helium as function of the drift parameter E/N . A theory based on the mean hard-sphere cross section and the ion-induced dipole interactions was used to predict the zero-field reduced mobilities. Good agreement between the theoretical predictions and experimental results of ion mobilities validates the reliability of quantum chemical calculations of the optimised ion geometries which can be further employed for molecular dynamics simulations of the mechanism of proton transfer collisions between H_3O^+ and VOCs.

Acknowledgements. GAČR project: “Selected ion flow drift tube mass spectrometry with negative ions and nitrogen carrier gas” 21-25486S.

References

- Bhatia, M., A DFT evaluation of molecular reactivity of volatile organic compounds in support of chemical ionization mass spectrometry, *Computational and Theoretical Chemistry*, 1223, 114101, 2023.
- Bouchoux, G., J. Y. Salpin, and D. Leblanc, A relationship between the kinetics and thermochemistry of proton transfer reactions in the gas phase, *Int. J. Mass Spectrom. Ion Process.*, 153 (1), 37–48, 1996.
- Bruderer, T., T. Gaisl, M. T. Gaugg, N. Nowak, B. Streckenbach, S. Muller, A. Moeller, M. Kohler, and R. Zenobi, On-Line Analysis of Exhaled Breath, *Chem. Rev.*, 119 (19), 10803–10828, 2019.
- Caldeweyher, E., C. Bannwarth, and S. Grimme, Extension of the D3 dispersion coefficient model, *The Journal of Chemical Physics*, 147 (3), 034112, 2017.
- Dryahina, K., and P. Španěl, A convenient method for calculation of ionic diffusion coefficients for accurate selected ion flow tube mass spectrometry, SIFT-MS, *Int. J. Mass Spectrom.*, 244 (2–3), 148–154, 2005.
- Ellis, H. W., E. W. McDaniel, D. L. Albritton, L. A. Viehland, S. L. Lin, and E. A. Mason, Transport properties of gaseous ions over a wide energy range. Part II, *At. Data Nucl. Data Tables*, 22 (3), 179–217, 1978.
- Etim, E. E., O. E. Godwin, and S. A. Olagboye, Protonation in Hydrocarbons: Allene (C_3H_4), Isobutane (C_4H_{10}), 2-butyne (CH_3CCCH_3), 1, 2-butadiene and 1, 3-butadiene C_4H_6 , *International Journal of Advanced Research in Chemical Science*, 7 (3), 11–22, 2020.
- Hanwell, M. D., D. E. Curtis, D. C. Lonie, T. Vandermeersch, E. Zurek, and G. R. Hutchison, Avogadro: an advanced semantic chemical editor, visualization, and analysis platform, *J. Cheminform.*, 4, 17, 2012.
- Hunter, E. P. L., and S. G. Lias, Evaluated Gas Phase Basicities and Proton Affinities of Molecules: An Update, *J. Phys. Chem. Ref. Data*, 27 (3), 413–656, 1998.

- Kim, S., J. Chen, T. Cheng, A. Gindulyte, J. He, S. He, Q. Li, B. A. Shoemaker, P. A. Thiessen, B. Yu, L. Zaslavsky, J. Zhang, and E. E. Bolton, PubChem 2023 update, *Nucleic Acids Research*, 51 (D1), D1373–D1380, 2022.
- Lias, S. G., R. D. Levin, and S. A. Kafafi, “Ion Energetics Data” in NIST Chemistry WebBook, NIST Standard Reference Database Number 69. In *National Institute of Standards and Technology*, Gaithersburg, 2016.
- McDaniel, E. W., and E. A. Mason, *The Mobility and Diffusion of Ions in Gases*. John Wiley: New York, 1973.
- Neese, F., Software update: the ORCA program system, version 4.0, *Wiley Interdisciplinary Reviews-Computational Molecular Science*, 8 (1), 2018.
- Linstrom, P. J., W. G. Mallard, NIST Chemistry WebBook, NIST Standard Reference Database Number 69, In *National Institute of Standards and Technology*, Gaithersburg, 2011.
- Spesvyi, A., D. Smith, and P. Španěl, Selected Ion Flow-Drift Tube Mass Spectrometry: Quantification of Volatile Compounds in Air and Breath, *Anal. Chem.*, 87 (24), 12151–12160, 2015.
- Spesvyi, A., and P. Španěl, Determination of residence times of ions in a resistive glass selected ion flow-drift tube using the Hadamard transformation, *Rapid Commun. Mass Spectrom.*, 29 (17), 1563–1570, 2015.
- Spesvyi, A., M. Lacko, K. Dryahina, D. Smith, and P. Španěl, Ligand Switching Ion Chemistry: An SIFDT Case Study of the Primary and Secondary Reactions of Protonated Acetic Acid Hydrates with Acetone, *J. Am. Soc. Mass Spectrom.*, 32 (8), 2251–2260, 2021.
- Tichy, M., G. Javahery, N. D. Twiddy, and E. E. Ferguson, The Application of a Selected-Ion Flow Drift Tube to the Determination of Proton Affinity Differences, *Int. J. Mass Spectrom. Ion Process.*, 93 (2), 165–175, 1989.
- Tichý, M., N. D. Twiddy, D. P. Wareing, N. G. Adams, and D. Smith, Sifdt Studies of the Reactions of N_4^+ Ions with H_2 , D_2 , and Ar, *Int. J. Mass Spectrom. Ion Process.*, 81, 235–246, 1987.
- Zare, R. N., F. M. Fernandez, and J. R. Kimmel, Hadamard transform time-of-flight mass spectrometry: More signal, more of the time, *Angew. Chem.-Int. Edit.*, 42 (1), 30–35, 2003.